

Top Decays with Flavor Changing Neutral Higgs Interactions at the LHC

Chung Kao^{a,b*}, Hai-Yang Cheng^{b†}, Wei-Shu Hou^{c‡}, and Joshua Sayre^{a§}

^a*Homer L. Dodge Department of Physics and Astronomy,
University of Oklahoma, Norman, OK 73019, USA*

^b*Institute of Physics, Academia Sinica, Taipei 11529, Taiwan, ROC*

^c*Department of Physics, National Taiwan University, Taipei 10617, Taiwan, ROC*

(Dated: April 22, 2019)

Abstract

We investigate the prospects for the discovery of a top quark decaying into one light Higgs boson along with a charm quark in top quark pair production at the CERN Large Hadron Collider (LHC). A general two Higgs doublet model is adopted to study the signature of flavor changing neutral Higgs interactions for $t \rightarrow c\phi^0$ or $\bar{t} \rightarrow \bar{c}\phi^0$ where ϕ^0 is a CP-even scalar (H^0) or a CP-odd pseudoscalar (A^0). The dominant physics background is evaluated with realistic acceptance cuts as well as tagging and mistagging efficiencies. We have found abundant signal events and that our acceptance cuts reduce the physics background enough to establish a 5σ signal for $M_\phi \lesssim 130$ GeV at the early stage of LHC with $\sqrt{s} = 7$ TeV and an integrated luminosity of 10 fb^{-1} . The discovery potential will be greatly enhanced with the full energy of $\sqrt{s} = 14$ TeV.

PACS numbers: 12.60.Fr, 12.15Mm, 14.80.Ec, 14.65.Ha

* E-mail address: kao@physics.ou.edu

† E-mail address: phcheng@phys.sinica.edu.tw

‡ E-mail address: wshou@phys.ntu.edu.tw

§ E-mail address: sayre@physics.ou.edu

I. INTRODUCTION

The Standard Model has been very successful in explaining almost all experimental data to date, culminating in the discovery of the top quark [1, 2] and the tau neutrino [3]. The most important experimental goals of the CERN Large Hadron Collider (LHC) are the investigation of the mechanism for electroweak symmetry breaking (EWSB)—the discovery of the Higgs bosons or the proof of their non-existence, and the search for new physics beyond the Standard Model.

In the Standard Model (SM) there is one Higgs doublet, which generates masses for vector bosons and fermions. The differences among Yukawa couplings of fermions with the Higgs boson are not explained. In addition, there are no flavor changing neutral currents (FCNC) mediated by gauge interactions or by Higgs interactions at the tree level.

At present, the top quark is the most massive elementary particle ever discovered. It might provide clues to study the mechanisms of EWSB and FCNC. A general two Higgs doublet model usually contains flavor changing neutral Higgs (FCNH) vertices if there is no discrete symmetry to turn off tree-level FCNC [4, 5]. Furthermore, a special two Higgs doublet model for the top quark (T2HDM) [6] offers a good explanation of why the top quark is much heavier than other elementary particles. In the T2HDM, the top quark is the only elementary fermion acquiring its mass from a special Higgs doublet (ϕ_2) with a large vacuum expectation value (VEV). Since the up and the charm quarks couple to another Higgs doublet (ϕ_1), there are FCNH interactions among the up-type quarks.

In the near future, the LHC will produce approximately 1.6×10^6 top quark pairs ($t\bar{t}$) [7–9] for $m_t \simeq 173$ GeV and an integrated luminosity of $\mathcal{L} = 10 \text{ fb}^{-1}$ at $\sqrt{s} = 7$ TeV. For the same integrated luminosity at $\sqrt{s} = 14$ TeV it will be able to generate about 1×10^7 ($t\bar{t}$) pairs. That means, the LHC will become a top quark factory providing great opportunities to study electroweak symmetry breaking as well as other important properties of the top quark. If the top quark is heavier than a neutral Higgs boson that interacts with a top quark and a charm quark, then a promising FCNH signature will appear in pp collisions as $pp \rightarrow t\bar{t} \rightarrow t\bar{c}\phi^0 + X$ or $pp \rightarrow t\bar{t} \rightarrow c\phi^0\bar{t} + X$ at the LHC [10].

In this letter, we study the discovery potential of the LHC in the search for the rare top decay $t \rightarrow c\phi^0$, where ϕ^0 is a scalar (H^0) or a pseudoscalar (A^0). The Higgs boson then decays into a pair of bottom quarks ($b\bar{b}$). We have evaluated production rates with full tree-level matrix elements including Breit-Wigner resonances for both the signal and the physics background. In addition, we optimize the acceptance cuts to effectively reduce the background with realistic b -tagging and mistagging efficiencies. Promising results are presented for the LHC with $\sqrt{s} = 7$ TeV as well as $\sqrt{s} = 14$ TeV. Section II shows the production cross sections for the Higgs signal and the dominant background as well as our strategy to determine the reconstructed masses for the top quark and the Higgs boson. Realistic acceptance cuts are discussed in Section III. Section IV presents the discovery potential at the LHC for $\sqrt{s} = 7$ TeV and $\sqrt{s} = 14$ TeV. Optimistic conclusions are drawn in Section V.

II. THE HIGGS SIGNAL AND THE PHYSICS BACKGROUND

A. The Higgs Signal

We adopt a general two Higgs doublet model to study flavor changing neutral Higgs interactions with the following effective Lagrangian

$$\mathcal{L} = -\lambda_{tc}\bar{c}tH^0 - i\lambda_{tc}\bar{c}\gamma_5 tA^0 + \text{H.c.} \quad (1)$$

where H^0 is a CP-even scalar, A^0 is a CP-odd pseudoscalar and $v = 2M_W/g_W \simeq 246$ GeV. For $M_\phi < m_t$, the $t \rightarrow c\phi^0$ decay width [11] is

$$\Gamma(t \rightarrow c\phi^0) = \frac{|\lambda_{tc}|^2}{16\pi} \times (m_t) \times [(1 \pm \rho_c)^2 - \rho_\phi^2] \times \sqrt{1 - (\rho_\phi + \rho_c)^2} \sqrt{1 - (\rho_\phi - \rho_c)^2} \quad (2)$$

where $\phi^0 = H^0$ or A^0 , $\rho_c = m_c/m_t$, $\rho_\phi = M_\phi/m_t$, and $+$ or $-$ corresponds to ϕ^0 being a scalar or a pseudoscalar. We assume that the total decay width of the top quark is

$$\Gamma_t = \Gamma(t \rightarrow bW) + \Gamma(t \rightarrow c\phi^0). \quad (3)$$

Then the branching fraction of $t \rightarrow c\phi^0$ becomes

$$\mathcal{B}(t \rightarrow c\phi^0) = \frac{\Gamma(t \rightarrow c\phi^0)}{\Gamma_t}. \quad (4)$$

As a case study, we take the FCNH Yukawa couplings to be the geometric mean of the Yukawa couplings of the quarks¹ [12, 13]

$$\lambda_{tc} = \frac{\sqrt{m_t m_c}}{v} \simeq 0.063 \quad (5)$$

with $m_t = 173.3$ GeV and $m_c = 1.4$ GeV. Then the branching fraction of $t \rightarrow c\phi^0$ becomes $\mathcal{B}(t \rightarrow c\phi^0) = 2.6 \times 10^{-3}$ for $M_\phi = 120$ GeV or $\mathcal{B}(t \rightarrow c\phi^0) = 6.2 \times 10^{-4}$ for $M_\phi = 150$ GeV. For illustration we use this ansatz in all our figures except for Fig. 5. Later, in the section on LHC discovery potential, we will consider λ_{tc} as a free parameter. We assume that the width and branching fraction of the Higgs scalar decay to $b\bar{b}$ are similar to those of the standard Higgs boson, while the Higgs pseudoscalar decays to the W^+W^- or ZZ pairs are negligible. We do not consider CP violation in this study.

We employ the programs MadGraph [14, 15] and HELAS [16] to evaluate the exact matrix element for the FCNH signal in top decays from gluon fusion and quark-antiquark annihilation, $gg \rightarrow t\bar{t} \rightarrow t\bar{c}\phi^0 \rightarrow b\ell^+\nu\bar{c}b\bar{b}$ and $q\bar{q} \rightarrow t\bar{t} \rightarrow t\bar{c}\phi^0 \rightarrow b\ell^+\nu\bar{c}b\bar{b}$ as well as $t\bar{t} \rightarrow c\phi^0\bar{t} \rightarrow cb\bar{b}\bar{b}\ell^-\bar{\nu}$, where $\ell = e$ or μ . The signal cross section at the LHC for $pp \rightarrow t\bar{t} \rightarrow tc\phi^0 \rightarrow b\ell\nu c\bar{b}\bar{b} + X$ is evaluated with the parton distribution functions of CTEQ6L1 [17]. In addition, we have checked the signal cross section by narrow width approximation. That means, the cross section $\sigma(pp \rightarrow t\bar{t} \rightarrow tc\phi^0 \rightarrow b\ell\nu c\bar{b}\bar{b} + X)$ is calculated as the product of cross section times branching fractions: $\sigma(pp \rightarrow t\bar{t} \rightarrow b\ell\nu\bar{t} + X) \times \mathcal{B}(t \rightarrow c\phi^0) \times \mathcal{B}(\phi^0 \rightarrow b\bar{b})$. The factorization scale and the renormalization scale are chosen to be $Q = \sqrt{s} = M_{t\bar{t}}$, that

¹ We note that some physicists choose the Yukawa coupling to be $y_{tc} = \sqrt{2}\lambda_{tc}$.

is, the invariant mass of $t\bar{t}$. This choice of scale leads to a K factor of 2 for top quark pair production [18, 19].

In our analysis, we consider the FCNH signal from both $t\bar{t} \rightarrow t\bar{c}\phi^0 \rightarrow b\ell^+\nu\bar{c}b\bar{b}$ and $t\bar{t} \rightarrow c\phi^0\bar{t} \rightarrow cb\bar{b}\bar{b}\ell^-\bar{\nu}$, which will be commonly described as $t\bar{t} \rightarrow c\phi^0\bar{t} \rightarrow cb\bar{b}\bar{b}\ell\nu$. In every event, we require there should be 3 b jets and one light jet ($j = u, d, s, c$, or g). In addition, there is an isolated lepton ($\ell = e$ or μ), and the neutrino will lead to missing transverse energy (\cancel{E}_T). Unless explicitly specified, q generally denotes a quark (q) or an anti-quark (\bar{q}) and ℓ will represent a lepton ℓ^- or anti-lepton (ℓ^+). That means our FCNH signal leads to the final state of $b\ell\nu b\bar{b}j$ or $bbbj\ell + \cancel{E}$.

B. The Physics Background

The dominant physics background to the final state of $bbbj\ell\nu$ comes from top quark pair production followed by top and W decays: $pp \rightarrow t\bar{t} \rightarrow b\ell^+\nu\bar{b}\bar{c}s + X$ or $pp \rightarrow t\bar{t} \rightarrow bc\bar{s}\bar{b}\ell^-\bar{\nu} + X$, where a c -jet is mis-identified as a b -jet. We have also considered backgrounds from $t\bar{t} \rightarrow b\ell\nu\bar{b}u\bar{d}$, as well as backgrounds from the production of $b\bar{b}\bar{b}\bar{b}\ell\nu$ and $b\bar{b}c\bar{c}\ell\nu$. According to the ATLAS and CMS Technical Design Reports [20, 21] the probability that a c -jet is mistagged as a b -jet (ϵ_c) is approximately 10%, while the probability that any other jet is mistagged as a b -jet (ϵ_j) is 1%. If ϵ_c is chosen to be the same as that of a light jet, the background will be underestimated by a factor of 10 such as in the analysis in Ref. [10].

C. Mass Reconstruction

In this subsection, we discuss our strategy to determine the reconstructed top mass as the invariant mass of M_{bbj} for the top quark with FCNC (t or $\bar{t} \rightarrow c\phi^0 \rightarrow cb\bar{b}$), as well as the other reconstructed top mass with leptonic decay (\bar{t} or $t \rightarrow bW \rightarrow b\ell\nu$):

$$M_{t_1}^R = M_{bbj}, \quad (6)$$

$$M_{t_2}^R = M_{b\ell\nu}. \quad (7)$$

In the process of doing so, we reconstruct the Higgs mass as the invariant mass of a pair of b jets and one W mass as the invariant mass of a charged -lepton/neutrino pair $\ell\nu$. We also reconstruct a potential second W mass from a b -jet/light jet pair for vetoing the background:

$$M_\phi^R = M_{bb}, \quad (8)$$

$$M_{W_1}^R = M_{bj}, \quad (9)$$

$$M_{W_2}^R = M_{\ell\nu}. \quad (10)$$

Figure 1 shows invariant mass distributions with basic cuts: $p_T(b, j) \geq 15$ GeV, $p_T(\ell) \geq 20$ GeV and $|\eta(b, j, \ell)| \leq 2.5$. In each event, we assume that three b jets and one non- b jet are identified through b -tagging. We then assign the three b jets (b_1, b_2, b_3) according to the following procedure: Since our FCNC signal comes from $t\bar{t} \rightarrow c\phi^0\bar{b}\ell\bar{\nu} \rightarrow b\bar{b}c\bar{b}\ell\bar{\nu} \rightarrow bbbj\ell + \cancel{E}$, we will choose the pair of b jets that minimize $|M_{bbj} - m_t|$ as b_1b_2 and label the other b jet as b_3 . For a correctly reconstructed event, b_1 and b_2 are the products of a Higgs decay as well, such that their invariant mass has a peak near M_ϕ . For a background event, one b is likely coming from the top decay $t \rightarrow bW \rightarrow bcj$ while the other is either a mistagged

c or a light quark jet coming from W decay, or a real b quark coming from the decay of \bar{t} . Let us identify b_2 as the member of this pair that minimizes $M_{bj} - m_W$. In a good reconstruction, the remaining b quark, b_3 should reproduce the top quark mass with the charged lepton and neutrino momenta. In this figure, we present the reconstructed masses for signal and background with $M_\phi = 120$ GeV: $M_{bbj} = M_{b_1b_2j} = M_{t_1}^R$, $M_{bb} = M_{b_1b_2} = M_\phi^R$, $M_{bj} = M_{b_2j} = m_{W_1}^R$, and $M_{b\ell\nu} = M_{b_3\ell\nu} = m_{t_2}^R$. We have used the Higgs pseudoscalar case here and in Fig. 2 as an example; the shapes are virtually the same for a scalar.

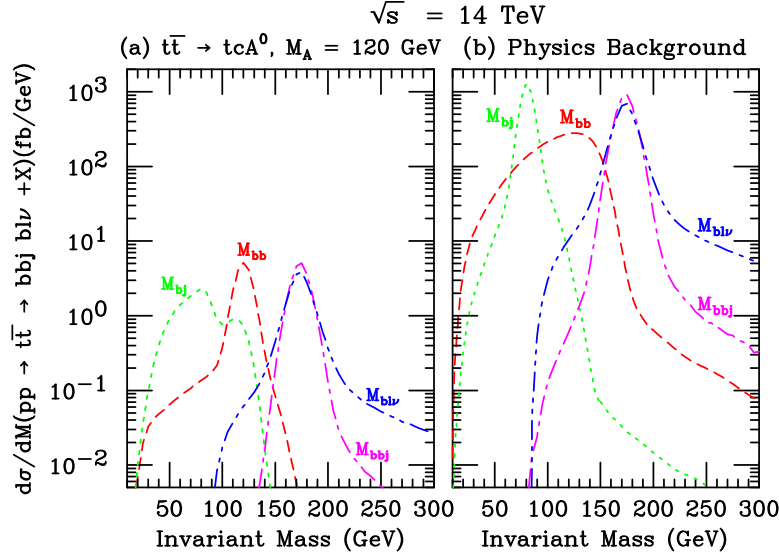


FIG. 1: Invariant mass distribution of bbj (dash-dot magenta), $b\ell\nu$ (dash-dot-dot blue), bb (dash red), and bj (dot green), with basic cuts on p_T and η for (a) the Higgs signal from $pp \rightarrow t\bar{t} \rightarrow tcA^0 \rightarrow b\ell\nu cb\bar{b} + X$ and (b) the Standard Model background from $pp \rightarrow t\bar{t} \rightarrow b\ell\nu bcs + X$ where q is a q or a \bar{q} .

In our analysis, we assume that the FCNH signal comes from top quark pair production with one top quark decaying via FCNC while the other decays leptonically ($t \rightarrow bW \rightarrow b\ell\nu$). For a real W decay ($W \rightarrow \ell\nu$), the momentum of the neutrino (k) and that of the lepton (p) have the following relation

$$(k + p)^2 = m_W^2. \quad (11)$$

If the missing transverse energy comes solely from the neutrino in W decay, we can estimate the longitudinal momentum of the neutrino (k_z) with measured lepton energy and momentum (E_ℓ, \vec{p}), transverse missing momentum ($k_x = \cancel{E}_x$ and $k_y = \cancel{E}_y$) and $E_\nu = |\vec{k}|$.

Assuming an on-shell W , we can evaluate k_z of the neutrino with

$$k_z = \frac{p_z[2(p_x k_x + p_y k_y) + m_W^2 - m_\ell^2] \pm E_\ell \Delta}{m_\ell^2 + p_T^2} \quad (12)$$

with

$$\Delta^2 = [2(p_x k_x + p_y k_y) + m_W^2 - m_\ell^2]^2 - 4k_T^2(m_\ell^2 + p_T^2). \quad (13)$$

There are two possible values for k_z if $\Delta^2 > 0$. We select whichever leads to a better reconstruction of the top-quark mass,

$$\text{Min}[m_t^2 - (k + p + p_{b_3})^2] \quad (14)$$

and define this reconstructed top mass as $M_{t_2}^R = M_{b_3\ell\nu}$. In case $\Delta^2 < 0$, we set $\Delta = 0$ to evaluate k_z , corresponding to a virtual W . We require that the reconstructed W mass ($M_{\ell\nu}$) should be close to the on-shell mass m_W .

III. REALISTIC ACCEPTANCE CUTS

To study the discovery potential of this FCNH signal at the LHC, we have applied realistic cuts and tagging efficiencies for three combinations of the CM energy (\sqrt{s}) and integrated luminosity (L): (a) the early stage of LHC with $\sqrt{s} = 7$ and $L = 10 \text{ fb}^{-1}$, (b) full CM energy ($\sqrt{s} = 14 \text{ TeV}$) with low luminosity $L = 30 \text{ fb}^{-1}$, and (c) full CM energy ($\sqrt{s} = 14 \text{ TeV}$) with high luminosity $L = 300 \text{ fb}^{-1}$.

For (a) the early LHC and (b) full CM energy with low luminosity, we require that in every event there should be

- exactly 4 jets that have $p_T > 15 \text{ GeV}$ and $|\eta| < 2.5$, and three of them must be tagged as b -jets;
- exactly one isolated lepton that has $p_T > 20 \text{ GeV}$ and $|\eta| < 2.5$;
- the missing transverse energy (\cancel{E}_T) must be greater than 20 GeV ;
- at least one pair of b -jets such that the invariant mass of $b_1 b_2 j$ should be near m_t : $|M_{b_1 b_2 j} - m_t| \leq 25 \text{ GeV}$;
- the pair of b -jets, $b_1 b_2$, that reconstructs the hadronically decaying top should also satisfy $|M_{b_1 b_2} - M_\phi| \leq 0.15 M_\phi$;
- a third b jet such that the invariant mass of $b_3 \ell \nu$ should be near m_t : $|M_{b_3 \ell \nu} - m_t| \leq 25 \text{ GeV}$;
- the reconstructed leptonic W must satisfy $|M_{\ell\nu} - m_W| \leq 15 \text{ GeV}$.

Additionally, to effectively reduce backgrounds from $W \rightarrow jj$, we require $|M_{b_2 j} - m_W| > 15 \text{ GeV}$. We also require $\Delta R = \sqrt{\Delta\phi^2 + \Delta\eta^2} > 0.4$ between every pair of jets and between each jet and the charged lepton, to limit QCD production of multi-jets and ensure good reconstruction of isolated jets and the charged lepton.

In the early stage of LHC with $\sqrt{s} = 7 \text{ TeV}$, the b -tagging efficiency (ϵ_b) is taken to be 50%, the probability that a c -jet is mistagged as a b -jet (ϵ_c) is 10% and the probability that any other jet is mistagged as a b -jet (ϵ_j) is taken to be 1%. At the full CM energy ($\sqrt{s} = 14 \text{ TeV}$) with an integrated luminosity (L) of 30 fb^{-1} , we follow the tagging and mistagging efficiencies in the ATLAS Technical Design Report [20]: $\epsilon_b = 60\%$, $\epsilon_c = 14\%$ and $\epsilon_j = 1\%$.

For the full CM energy ($\sqrt{s} = 14 \text{ TeV}$) with a high integrated luminosity of 300 fb^{-1} , we require $p_T(b, j) > 30 \text{ GeV}$, $p_T(\ell) > 20 \text{ GeV}$, $|\eta(b, j, \ell)| < 2.5$, and $\cancel{E} > 40 \text{ GeV}$. The tagging and mistagging efficiencies are taken to be $\epsilon_b = 50\%$, $\epsilon_c = 14\%$ and $\epsilon_j = 1\%$.

Furthermore, a powerful acceptance cut on the charm-jet energy was proposed in a study to search for FCNH top decays at linear colliders [22]. In the rest frame of the top quark, the energy of the charm jet from $t \rightarrow c\phi^0$ is

$$E_c^R = \frac{m_t}{2} \left(1 + \frac{m_c^2}{m_t^2} - \frac{M_\phi^2}{m_t^2} \right). \quad (15)$$

For $M_\phi = 120$ GeV, $E_c^R \simeq 45$ GeV, while for $M_\phi = 150$ GeV, $E_c^R \simeq 22$ GeV. In the background, the non- b jet, which is most likely not a charm quark and which arises from W decay, has a distribution of energy which is more spread out [22].

In Fig. 2, we present the distribution with respect to the charm energy in the top rest frame (E_c^R) for $pp \rightarrow t\bar{t} \rightarrow b\ell\nu c b\bar{b} + X$ with (a) $M_A = 120$ GeV and (b) $M_A = 150$ GeV. Also shown is the same distribution for the physics background from $pp \rightarrow t\bar{t} \rightarrow b\ell\nu bcs + X$ where the charm quark is mistagged as a b and the strange quark fakes a charm jet. In our complete analysis, we choose $35 \text{ GeV} < E_c^R < 55 \text{ GeV}$ for $M_\phi = 120$ GeV, and $12 \text{ GeV} < E_c^R < 32 \text{ GeV}$ for $M_\phi = 150$ GeV.

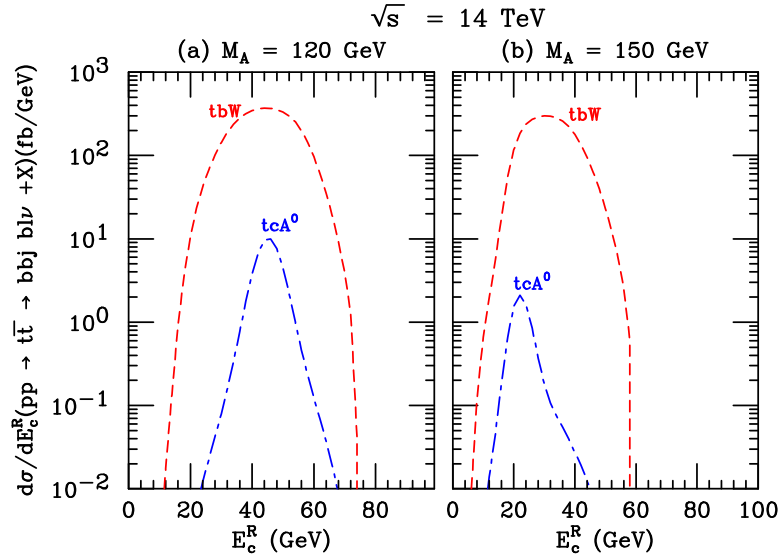


FIG. 2: Distribution with respect to the charm energy in the top rest frame (E_c^R) $pp \rightarrow t\bar{t} \rightarrow b\ell\nu c b\bar{b} + X$ (dot-dash blue) for (a) $M_A = 120$ GeV and (b) $M_A = 150$ GeV. Also shown is the same distribution for the physics background from $pp \rightarrow t\bar{t} \rightarrow b\ell\nu bcs + X$ (dash red).

Measurement uncertainties in jet and lepton momenta as well as missing transverse momentum give rise to a spread in the reconstructed masses about the true values of m_t and M_ϕ . Based on the ATLAS [20] and the CMS [21] specifications we model these effects by Gaussian smearing of momenta:

$$\frac{\Delta E}{E} = \frac{0.60}{\sqrt{E(\text{GeV})}} \oplus 0.03 \quad (16)$$

for jets and

$$\frac{\Delta E}{E} = \frac{0.25}{\sqrt{E(\text{GeV})}} \oplus 0.01 \quad (17)$$

for charged leptons with individual terms added in quadrature.

IV. DISCOVERY POTENTIAL AT THE LHC

Our results for the signal and background at the LHC with $\sqrt{s} = 7$ TeV and $\sqrt{s} = 14$ TeV are presented in Figs. 3 and 4 respectively. To estimate the discovery potential at the LHC we include curves that correspond to the minimal cross section of signal (σ_S) required by our discovery criterion described in the following. We define the signal to be observable if the lower limit on the signal plus background is larger than the corresponding upper limit on the background [23] with statistical fluctuations

$$L(\sigma_S + \sigma_B) - N\sqrt{L(\sigma_S + \sigma_B)} \geq L\sigma_B + N\sqrt{L\sigma_B} \quad (18)$$

or equivalently,

$$\sigma_S \geq \frac{N}{L} \left[N + 2\sqrt{L\sigma_B} \right]. \quad (19)$$

Here L is the integrated luminosity, σ_S is the cross section of the FCNH signal, and σ_B is the background cross section. The parameter N specifies the level or probability of discovery. We take $N = 2.5$, which corresponds to a 5σ signal.

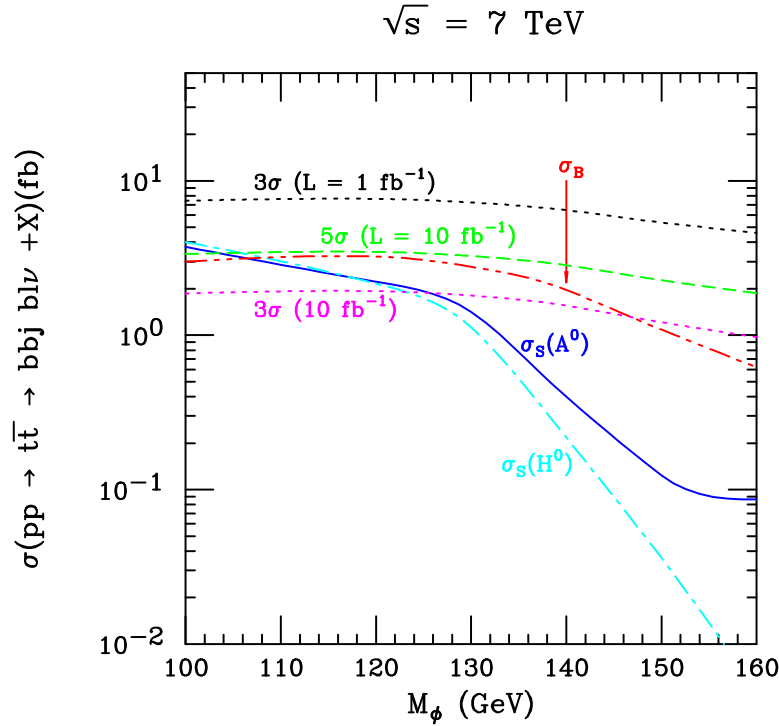


FIG. 3: The cross section of $pp \rightarrow t\bar{t} \rightarrow t\bar{t}\phi^0 \rightarrow b\ell\nu c b\bar{b} + X$ at the LHC with $\sqrt{s} = 7$ TeV, as a function of M_ϕ . We present results for Higgs scalar H^0 (dash-dot cyan) and Higgs pseudoscalar A^0 (solid blue). Also shown are the background cross section (dash-dot-dot red) and the thresholds for 5σ discovery with 10 fb^{-1} (dash green) of integrated luminosity, or 3σ evidence with 10 fb^{-1} (dot magenta) or 1 fb^{-1} (dot black). We take the ansatz of Eq. (5) to set the FCNH coupling strength and have applied K factors, acceptance cuts, and efficiencies of b -tagging and mistagging.

For $L\sigma_B \gg 1$, this requirement becomes similar to

$$N_{\text{SS}} = \frac{N_S}{\sqrt{N_B}} = \frac{L\sigma_S}{\sqrt{L\sigma_B}} \geq 5, \quad (20)$$

where N_S is the signal number of events, N_B is the background number of events, and N_{SS} is the statistical significance, which is commonly used in the literature. If the background has fewer than 25 events for a given luminosity, we employ the Poisson distribution and require that the Poisson probability for the SM background to fluctuate to this level is less than 2.85×10^{-7} , i.e. an equivalent probability to a 5-sigma fluctuation with Gaussian statistics.

Figure 3 shows the signal and background cross sections for the CERN Large Hadron Collider with $\sqrt{s} = 7$ TeV. All tagging efficiencies and K factors discussed above are included. As can be seen from the figure, with 10 fb^{-1} of data at 7 TeV running we can potentially discover this FCNC decay mode for a Higgs with mass less than ~ 106 GeV. We can establish a 3σ discrepancy from the Standard Model for masses below ~ 124 GeV. If the 2012 run of the LHC continues at $\sqrt{s} = 7$ TeV we may have $\sim 20 \text{ fb}^{-1}$ for each detector at the end of that year. One can estimate the sensitivity for this integrated luminosity by lowering the (10 fb^{-1}) 3σ and 5σ threshold lines by a factor of $\sqrt{2}$. At high masses the pseudoscalar signal is somewhat larger than the scalar case. This is due to the absence of W^+W^- and ZZ branching modes in the pseudoscalar decay.

In Fig. 4, we display the signal and background cross sections for the CERN Large Hadron Collider with $\sqrt{s} = 14$ TeV. We present a lower luminosity case (LL) with 30 fb^{-1} of data and a long-term high-luminosity case (HL) with 300 fb^{-1} . Cuts and tagging efficiencies are as described above.

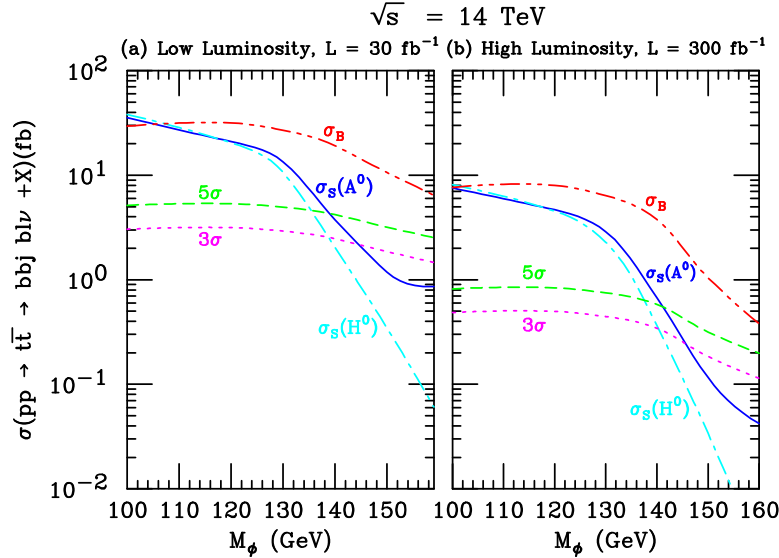


FIG. 4: The cross section of $pp \rightarrow t\bar{t} \rightarrow t c \phi^0 \rightarrow b l \nu c b \bar{b} + X$ at the LHC with $\sqrt{s} = 14$ TeV, as a function of M_ϕ . We present results for Higgs scalar H^0 (dash-dot cyan) and Higgs pseudoscalar A^0 (solid blue) with (a) $L = 30 \text{ fb}^{-1}$ and (b) $L = 300 \text{ fb}^{-1}$. Also shown are the background cross section (dash-dot-dot red) and the thresholds for 5σ discovery (dash green) or 3σ evidence (dot magenta). We take the ansatz of Eq. (5) to set the FCNH coupling strength and have applied K factors, acceptance cuts, and efficiencies of b -tagging and mistagging.

For $\sqrt{s} = 14$ TeV and $L = 30 \text{ fb}^{-1}$, the range for discovery is extended up to $M_H \sim 135$

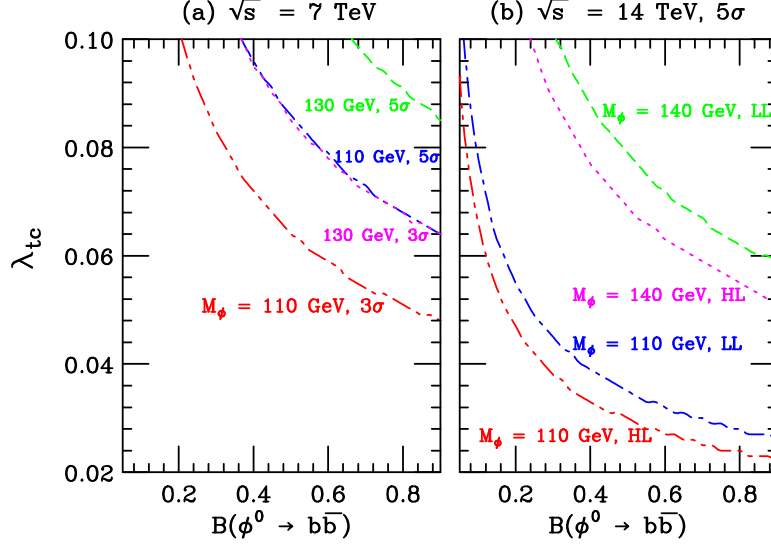


FIG. 5: The 5σ discovery contours at the LHC in the plane of $[\lambda_{tc}, \mathcal{B}(\phi^0 \rightarrow b\bar{b})]$ for (a) $M_\phi = 110$ GeV (dash-dot blue) or 130 GeV (dash green) at $\sqrt{s} = 7$ TeV and $L = 10 \text{ fb}^{-1}$, and (b) $M_\phi = 110$ GeV (LL: dash-dot blue, HL: dash-dot-dot red) or 140 GeV (LL: dash green, HL: dot magenta) with $\sqrt{s} = 14$ TeV and $L = 30 \text{ fb}^{-1}$ (LL) or 300 fb^{-1} (HL). For $\sqrt{s} = 7$ TeV, we also present curves for 3σ evidence, (dash-dot-dot red and dot magenta for $M_\phi = 110$ and 130 GeV respectively). The discovery region is the part of the parameter space above the contours.

GeV for a scalar coupling or $M_A \sim 138$ GeV for a pseudoscalar. With a high luminosity $L = 300 \text{ fb}^{-1}$, these ranges can be slightly improved to $M_H \sim 138$ GeV and $M_A \sim 142$ GeV respectively. High luminosity does not extend our range much, owing to (a) the kinematic limitations as the Higgs mass is increased towards the top mass, and (b) the higher p_T cuts and lower tagging efficiency we assume.

Figure 5 shows some discovery contours at the LHC for (a) $M_\phi = 110$ GeV or $M_\phi = 130$ GeV at $\sqrt{s} = 7$ TeV, and (b) $M_\phi = 110$ GeV or $M_\phi = 140$ GeV at $\sqrt{s} = 14$ TeV, as a function of the effective FCNH coupling λ_{tc} and the Higgs to $b\bar{b}$ branching fraction. These values of Higgs mass are chosen to demonstrate the possible mass range that might lead to promising FCNH signals.

V. CONCLUSIONS

It is a generic possibility of particle theories beyond the standard model to have contributions to tree-level FCNCs, especially for the third generation quarks. These contributions arise naturally in models with additional Higgs doublets, such as the T2HDM, wherein the top quark uniquely couples to one doublet. For a Higgs boson with a mass below the top mass, this could engender the rare decay $t \rightarrow c\phi^0$.

We investigated the prospects for discovering such a decay at the LHC, focusing on the channel where $t\bar{t}$ are pair produced and subsequently decay, one leptonically and one through the FCNC mode. The primary background for this signal is a $t\bar{t}$ pair with one standard hadronic decay and the other leptonic. This background involves one jet mis-tagged as a b jet, which is much more likely to occur for a c quark than for lighter jets. Nonetheless, by

taking advantage of the available kinematic information, one can reconstruct the resonances of the signal and reject much of the background.

Based on a simple geometric ansatz for the size of the FCNC coupling, we find that such a decay mode may be discovered at the LHC for Higgs masses up to 106 GeV with the current running energy and up to almost 140 GeV with the design energy of 14 TeV. We also presented results where the Higgs branching fraction and FCNC coupling are allowed to vary for fixed masses.

Recently, the ATLAS and the CMS experiments have made enormous progress on direct searches for the standard Higgs at the LHC. The SM Higgs boson has been excluded at 95% confidence level in the mass range 141–476 GeV [24]. We look forward to being guided by more new experimental results as we explore interesting physics of EWSB and FCNH.

Acknowledgments

We are grateful to Paoti Chang for beneficial discussions. C.K. thanks the Institute of Physics at the Academia Sinica for hospitality and support during a sabbatical visit. This research was supported in part by the U.S. Department of Energy under Grant No. DE-FG02-04ER41305, and by the National Science Council under Grant of Taiwan, R.O.C under Grant No. NSC-100-2112-M-001-009-MY3 (Academia Sinica). WSH thanks the National Science Council for Academic Summit grant NSC 100-2745-M-002 -002 -ASP.

Appendix: Comparison of Production Rates

In this appendix, we present production rates for the FCNH signal and the dominant background with the same parton distribution functions (MRST98 Set A [25]), the same cuts, and the same efficiencies ($\epsilon_b = 0.5$, $\epsilon_c = \epsilon_j = 0.01$) and the same K-factors, used in Ref. [10]. For the numerical analysis summarized below, we have adopted the same parameter $g_{tc} = 0.2$ or $\lambda_{tc} \simeq 0.046$ and the same branching fraction $\mathcal{B}(H \rightarrow b\bar{b}) = 0.7$. Our results are consistently lower, especially the Higgs signal, although we have tried to exactly reproduce their method.

TABLE I: Comparison of our number of events with results of Aguilar-Saavedra & Branco (in parentheses) calculated with the same cuts, efficiencies, PDFs and scales. c.f. Table 2 in Ref. [10].

| | Low Luminosity (10 fb ⁻¹) | | High Luminosity (100 fb ⁻¹) | |
|------------|---------------------------------------|---------------|---|---------------|
| | Before Cuts | Standard Cuts | Before Cuts | Standard Cuts |
| Signal | 200 (267) | 51.4 (98.2) | 1630 (2150) | 417 (797) |
| $t\bar{t}$ | 5491 (7186) | 24.7 (33.2) | 44540 (58230) | 198 (270) |
| $Wbbjj$ | 58 (77) | 0.22 (0.3) | 476 (644) | 1.7 (2.2) |

-
- [1] F. Abe *et al.* [CDF Collaboration], Phys. Rev. Lett. **74**, 2626 (1995).
 - [2] S. Abachi *et al.* [D0 Collaboration], Phys. Rev. Lett. **74**, 2632 (1995).
 - [3] K. Kodama *et al.* [DONUT Collaboration], Phys. Lett. **B504**, 218 (2001).
 - [4] S. L. Glashow and S. Weinberg, Phys. Rev. D **15**, 1958 (1977).
 - [5] J. F. Gunion, H. E. Haber, G. L. Kane and S. Dawson, Front. Phys. **80**, 1 (2000); *The Higgs Hunter's Guide* (Addison-Wesley, Redwood City, CA, 1990).
 - [6] A. K. Das and C. Kao, Phys. Lett. B **372**, 106 (1996).
 - [7] N. Kidonakis, Phys. Rev. D **82**, 114030 (2010).
 - [8] V. Ahrens, M. Neubert, B. D. Pecjak, A. Ferroglia and L. L. Yang, Phys. Lett. B **703**, 135 (2011).
 - [9] M. Cacciari, M. Czakon, M. L. Mangano, A. Mitov and P. Nason, arXiv:1111.5869 [hep-ph].
 - [10] J. A. Aguilar-Saavedra and G. C. Branco, Phys. Lett. B **495**, 347 (2000).
 - [11] W.-S. Hou, Phys. Lett. B **296**, 179 (1992).
 - [12] H. Fritzsch, Phys. Lett. B **73**, 317 (1978).
 - [13] T. P. Cheng and M. Sher, Phys. Rev. D **35**, 3484 (1987).
 - [14] T. Stelzer and W. F. Long, Comput. Phys. Commun. **81**, 357 (1994).
 - [15] J. Alwall *et al.*, JHEP **0709**, 028 (2007).
 - [16] H. Murayama, I. Watanabe and K. Hagiwara, “HELAS: HELicity amplitude subroutines for Feynman diagram evaluations,” KEK report KEK-91-11 (1991).
 - [17] J. Pumplin, D. R. Stump, J. Huston, H. L. Lai, P. Nadolsky and W. K. Tung, JHEP **0207**, 012 (2002).
 - [18] R. Bonciani, S. Catani, M. L. Mangano and P. Nason, Nucl. Phys. B **529**, 424 (1998) [Erratum-*ibid.* B **803**, 234 (2008)].
 - [19] P. Nason, S. Dawson and R. K. Ellis, Nucl. Phys. B **303**, 607 (1988).
 - [20] ATLAS Collaboration, “ATLAS Detector and Physics Performance Technical Design Report, CERN/LHCC 99-14/15 (1999)”; G. Aad *et al.* [The ATLAS Collaboration], “Expected Performance of the ATLAS Experiment - Detector, Trigger and Physics,” (2009).
 - [21] G. L. Bayatian *et al.* [CMS Collaboration], “CMS technical design report, volume II: Physics performance,” J. Phys. G **34**, 995 (2007).
 - [22] T. Han, J. Jiang and M. Sher, Phys. Lett. **B516**, 337 (2001).
 - [23] H. Baer, M. Bisset, C. Kao and X. Tata, Phys. Rev. D **46**, 1067 (1992).
 - [24] The ATLAS and the CMS Collaborations, “Combined Standard Model Higgs boson searches with up to 2.3 inverse femtobarns of pp collision data at $\sqrt{s}=7$ TeV at the LHC”, ATLAS-CONF-2011-157; CMS-PAS-HIG-11-023 (2011).
 - [25] A. D. Martin, R. G. Roberts, W. J. Stirling and R. S. Thorne, Eur. Phys. J. C **4**, 463 (1998).